International Endodontic Journal

doi:10.1111/j.1365-2591.2009.01595.x

An *in vivo* experimental model to assess furcal lesions as a result of perforation

M. J. B. Silva[1], M. V. Caliari[3], A. P. R. Sobrinho[2], L. Q. Vieira[1] & R. M. E. Arantes[3]

[1]Departamento de Bioquímica e Imunologia, Instituto de Ciências Biológicas, Universidade Federal de Minas Gerais, Belo Horizonte, MG, Brazil; [2]Departamento de Odontologia Restaurativa, Faculdade de Odontologia, Universidade Federal de Minas Gerais, Belo Horizonte, MG, Brazil; and [3]Departmento de Patologia Geral, Instituto de Ciências Biológicas, Universidade Federal de Minas Gerais, Belo Horizonte, MG, Brazil

Abstract

Silva MJB, Caliari MV, Sobrinho APR, Vieira LQ, Arantes RME. An *in vivo* experimental model to assess furcal lesions as a result of perforation. *International Endodontic Journal*, **42**, 922–929, 2009.

Aim To design and validate a rat molar model of furcal perforation to allow investigation of the biological phenomena that follow and to explore its potential for evaluating repair materials under standardized conditions.

Methodology Eighteen male Wistar rats were used. Surgical aseptic procedures were carried out in order to open the pulp chamber of a first molar tooth. A cavity was prepared on the floor of the pulp chamber using a ¼ round bur that created a communication between the furcation and the periodontal tissues. Six animals for each time point were sacrificed on days 14, 21 and 28 to assay morphological changes at the furcation region of molars. Maxillary bone was processed, removed and sectioned. Cellular infiltration, collagen deposition and bone resorption were assessed by histological analysis. Cellularity in the lesion area was determined by morphometric analysis. Data were analysed using parametric Student's *t*-test.

Results A furcal perforation model was standardized in which both radiological outcome and periodontal tissue reactions could be assessed through evaluation of cellularity, osteoclast activity and collagen deposition. The morphometric analysis revealed a greater number of cells 21 day post-surgery when compared with 14 days.

Conclusion This animal model was suitable for radiological and histological evaluation of the processes that accompany surgical furcal perforation.

Keywords: animal models, biomaterials, furcal perforations.

Received 3 September 2008; accepted 14 April 2009

Introduction

Accidental root canal or furcal perforation complicates the treatment and compromises the outcome of root canal treatment (Seltzer & Bender 1990, Walton & Torabinejad 2002). The prognosis of treatment of perforations is dependent on site, size, setting time of the repair material, and the efficacy of the material in terms of to seal (Walton & Torabinejad 2002). All of these factors are related to the ability to prevent or eliminate bacterial infiltration (Daoudi & Saunders 2002).

The chronic inflammatory reaction after accidental furcal perforation has been the object of several studies (Bhaskar & Rappaport 1971, Meister *et al.* 1979, Beavers *et al.* 1986, Seltzer & Bender 1990, Balla *et al.* 1991, Arens & Torabinejad 1996, Wu *et al.* 2005, Vajrabhaya *et al.* 2006, Al-Daafas & Al-Nazhan 2007,). This inflammatory reaction provokes alveolar bone damage around the perforation site where bone is progressively substituted by granulation tissue. The

Correspondence: Rosa Maria Esteves Arantes, MD, PhD, Laboratório de Neuro-imunopatologia Experimental, Departamento de Patologia Geral, Instituto de Ciências Biológicas, Universidade Federal de Minas Gerais, Av. Antônio Carlos, 6627, 31270-901, Belo Horizonte, MG, Brazil (Tel.: +5531 3409 2896/2884; fax: +5531 3409 2879; e-mail: rosa@icb.ufmg.br).

lack of bone tissue leads to loss of periodontal attachment that can affect tooth stability (Arens & Torabinejad 1996, Wu *et al.* 2005, Vajrabhaya *et al.* 2006, Al-Daafas & Al-Nazhan 2007).

Accidental furcal perforation has stimulated evaluation of the immunological responses that occur in the periodontal tissues and also the materials to seal the defects. It is believed that an ideal sealing material should seal the communication between the periodontium and pulp chamber and, at the same time, be biocompatible so as to induce bone and cement deposition (Hartwell & England 1993, Bernabé & Holland 2004). However, so far no ideal sealing material has been available.

To evaluate the prognosis and the best treatment choice different animal models have been used. Small rodents have many advantages as experimental models: (i) age and genetic rodent background can be well defined; (ii) better cost benefits; (iii) mouse and rats may be kept in controlled environments easily; (iv) there is a wide variety of gene knockout models. The rat bears much resemblance to man with respect to periodontal anatomy, development and composition of dental plaque, histopathology of periodontal lesions, and basic immunobiology (Klausen 1991). In this context, the characterization of alternative rodent models for dental research is important. Therefore, this study aimed at describing a new model to evaluate the outcome of furcal perforation including histopathological aspects using rats as the experimental model.

Material and methods

Animals

Wistar male rats weighing 240–260 g were obtained from CEBIO (Centro de Bioterismo da UFMG, Belo Horizonte, MG, Brazil) and kept in a conventional animal house with barriers and controlled light cycle. The experimental protocol was approved by the institutional animal ethical committee (protocol number 097/04, CETEA – UFMG). Six rats were used for each time point: 14, 21 and 28 days after the surgical procedure. Three rats were used as controls.

Anaesthesia

All experimental procedures were carried out under general anaesthesia. Rats were injected intra-muscularly with 100 mg kg^{-1} of ketamine hydrochloride (Dopalen, Division Vetbrands Animal Health, Jacareí, SP, Brazil) and 10 mg kg^{-1} of Xilazine (Anasedan, Agribrands do Brasil Ltda, Paulínia, SP, Brazil). The absence of flick reflex to hindpaw interdigital skin stretch was documented before the beginning of surgical procedures.

Surgical procedures

All experimental procedures were carefully performed under aseptic condition to avoid contamination. The disinfection of the surgical field was accomplished as proposed by Möller (1966).

Access to the pulp chamber in the rat molar tooth was prepared via the occlusal surface using a number 33½ carbide bur (KG Sorensen, Barueri, SP, Brazil) coupled to a controlled rotation handpiece (Driller, São Paulo, SP, Brazil) under air cooling. Once the pulp was exposed, the roof of the chamber was removed with an Endo Z bur (Dentsply Maillefer®, Catanduva, SP, Brazil). Coronal pulp tissue was removed using an endodontic probe until the level of root canal orifices. Haemorrhage was controlled by irrigating the chamber with saline solution and by applying pressure with sterilized cotton balls. As soon as bleeding was controlled, the chamber was irrigated again with saline solution and dried with cotton pellets. Subsequently, a perforation was created in the centre of the pulp chamber floor towards the alveolar bone using a number ¼ carbide drill (KG Sorensen, Barueri, SP, Brazil). To standardize the depth of the perforation, a cursor was glued to the drill 1 mm from its tip; the width was limited to the bur diameter (0.5 mm). A layer of gutta percha was inserted on the pulp chamber floor, avoiding contact between the sealing material and the perforation site. Condensation of gutta-percha was accomplished with the endodontic plugger and the excess was removed and contoured using a Hollemback 3S (SS White, Rio de Janeiro, RJ, Brazil). The tooth was restored with silver amalgam that was burnished using Dycal instrument (SS White); finally, the waste materials was removed using sterilized cotton balls. Prior to sacrifice the integrity of the amalgam was checked under an endodontic microscopy (Alliance microscopia, Sao Paulo, SP, Brazil).

MTA sealing procedure: testing the model application

To evaluate if it would be feasible to seal the experimental perforation and to analyse the surrounding periodontium tissues, six animals had their perforations filled with grey MTA (Ângelus®, Londrina, PR, Brazil). This material was manipulated according to the

manufacturer's recommendation and inserted using a probe. Animals were killed on day 21 post-surgery.

A video animation was designed using the blender software (Blender Foundation, Amsterdam, the Netherlands) to represent the entire surgical procedure (see Video Clip S1 of Supporting Information).

Radiographic procedures

Prior to the sacrifice, the animals were anaesthetized and killed by decapitation on days 14, 21 and 28 after the procedure. The hemi-maxilla was removed and radiographs were taken using a dental X-ray unit (Bioatlant, Ribeirão Preto, SP, Brazil). The optimal exposure parameters were determined as 0.12 s (70 kVp, 10 mA). Ekta-speed plus X-ray film (Eastman Kodak Co, Rochester NY, USA) was placed and fixed on a wooden surface to avoid movement. Then, the buccal side of the maxillary bone was placed so that side faced the machine. To take the image, the X-ray cone was set perpendicular to the X-ray film and 5 cm from it.

Histological preparation

The hemi-maxillas were immersed to 10% buffered formalin for 72 h at room temperature. Demineralization was performed for 30 days in EDTA solution (10% and pH 7.2) (Merck; Darmstadt; Germany). After demineralization, the samples were washed in running tap water for 24 h. Restorations were removed from the access cavities and the tissues were routinely processed for paraffin embedding. The hemi-maxillas were embedded with the buccal side of molars facing the base of the paraffin block. Consecutive (buccal-lingual direction) sections of 5 μm encompassing the perforation of the furcation area and both mesial and distal roots were stained with Haematoxylin/Eosin (H&E) and Gomori's Trichome and used to assess inflammatory infiltration, periodontal ligament organization and bone resorption.

Morphometric analysis

The inflammatory cells infiltrating the tissue adjacent to the perforation area was quantified. Images taken from the furcal areas were used to assay quantitatively the longitudinal inflammatory cell infiltration that occurred around the perforation, as shown in Fig. 3.

Quantification of the inflammatory cells in the furca area was conducted from three images selected from the same animal. The images were obtained at 40× magnification through a JVC TK-1270-RGB adapted to a microscope and analysed using KS300 software built into a Kontron Elektronick/Carl Zeiss image analyzer (Caliari 1997). An automatic macro recorder assembler (an algorithm of the KS300 software) was elaborated for capture, image processing and segmentation, definition of morphometrical conditions and counts of all the cells detected in each image. Image processing techniques were applied. Segmentation permitted the separation of these nuclei from cytoplasm and other structures in the section, such as blood vessels and extracellular space. Consequently, a binary image was created containing just the nuclei and other spaces (Pacheco *et al.* 2008). The nucleus from the cellular types usually found in the furca area and newly recruited leukocytes were then counted. It was imperative that only connective tissue, excluding bone and root dentine were visualized. This approach limited the acquisition of more than three images. The measurements were made by an observer who was unaware of the nature of the tissue sample. Three nonoperated rats were used as reference of normal periodontal cellularity.

Statistical analysis

Statistical analysis of mean values of cellular numbers obtained by morphometry was carried out using parametric Student's *t*-test. Statistical significance was set at $P < 0.05$.

Results

Clinical aspects

After anaesthesia and prior to sacrifice the animals were submitted to clinical evaluation. Animals tolerated the surgical procedure well and did not have signs of distress, weight loss or oral swelling. Colour and texture of the gingival regions were not altered.

Radiographic assessments

Figure 1a represents the nonoperated furcation and its adjacent tissue. Radiographs were performed to allow visualization of bone rebsorption. Radiographs were effective in revealing the three molar teeth as well as their associated alveolar bone and periodontal ligament space (Fig. 1b). Radiographic analyses demonstrated the position of the perforation (Fig. 1c) and, in some animals, interdental crestal destruction. In perforation

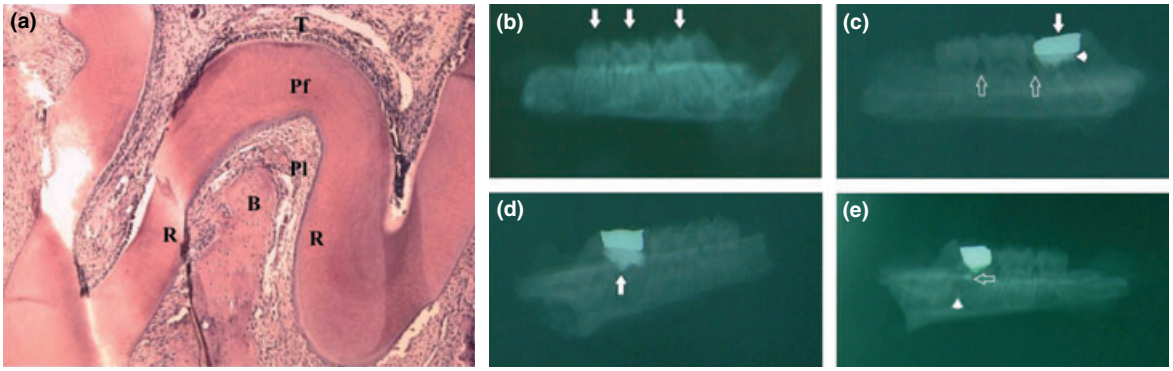

Figure 1 Histological aspect of the first left maxillary molar and radiograph aspects of tooth and periodontium tissue. (a) Panoramic normal histological aspect of the molar, (T, pulp tissue; PF, pulp chamber floor; PL, periodontal ligament; R, root; B, interradicular bone), H&E, ×40. (b) Radiological aspects of nonoperated group. White arrows mark the three molars. (c) Operated molar at day 14 post-surgery. White arrow marks the amalgam restoration. Note the gutta-percha material (arrow head). Open white arrow marks periodontal bone loss. (d) and (e) Operated and MTA-treated molar at day 21 post surgery. The white arrow represents MTA material sealing the furcal perforation. Note the MTA periodontium extrusion (open white arrow) and alveolar bone loss (arrow head).

sites sealed by MTA, radiographs demonstrated that it extended into the periodontal tissues (Fig. 1d,e).

Histopathology

Figure 2 shows the furcation area from operated animals on days 14, 21 and 28 post-surgery. On day 14, the periodontal ligament presented significant alterations in its architecture, showing intense cellular infiltration and edema, especially close to the perforation area (Fig. 2a). The following aspects were observed: mononuclear and polymorphonuclear cells prevailed in the underlying inflammatory infiltrate; edema interposition between tissue elements; intense vascular neoformation (Fig. 2b, inset); cement and root dentine reabsorption (Fig. 2f); intense collagen and connective tissue deposition and osteoclastic activity (Fig. 2f inset). On day 21 post-surgery, the samples showed chronic mononuclear inflammatory infiltrate around the perforation area. Collagen deposition was observed in the surrounding tissue apart from the perforation area (Fig. 2c). Fig. 2e represents samples from animals sacrificed 28 days after surgery. It shows a discrete chronic inflammatory infiltrate (Fig. 2e) and evidence of periodontal reorganization. In one sample, small necrotic areas surrounded by polymorphonuclear cells and debris were observed close to the deep bone layer, indicating that in some cases the surgical procedure resulted in bone microabscesses (data not show).

Figure 2d represents samples from rats that were killed on day 21 after surgery in which perforations were sealed by MTA. It demonstrates the presence of debris inside the perforation sites which could be MTA residue. The adjacent connective tissue presented a prevalence of mononuclear cells in the infiltrate, despite the presence of polymorphonuclear cells in some areas.

Morphometric analysis

As an example of quantitative analysis made possible by this model, we quantified the inflammatory cells infiltrating the tissue adjacent to the perforation area. Images taken from furcal area were used to assay quantitatively the longitudinal inflammatory cell infiltration that occurred around the perforation, as shown in Fig. 3. It was observed that cell numbers were much higher in furcal areas of operated animals than in animals that were not submitted to surgery.

Discussion

It is fundamental to the treatment of a perforation that the site does not become infected, and that it is sealed immediately. Prognosis of treatment depends on the perforation site, size of damage, adjacent periodontal condition and type of sealing material (Walton & Torabinejad 2002). The sealing ability of the material and its possible extrusion into the periodontal area should also be considered. Furthermore, good visibility

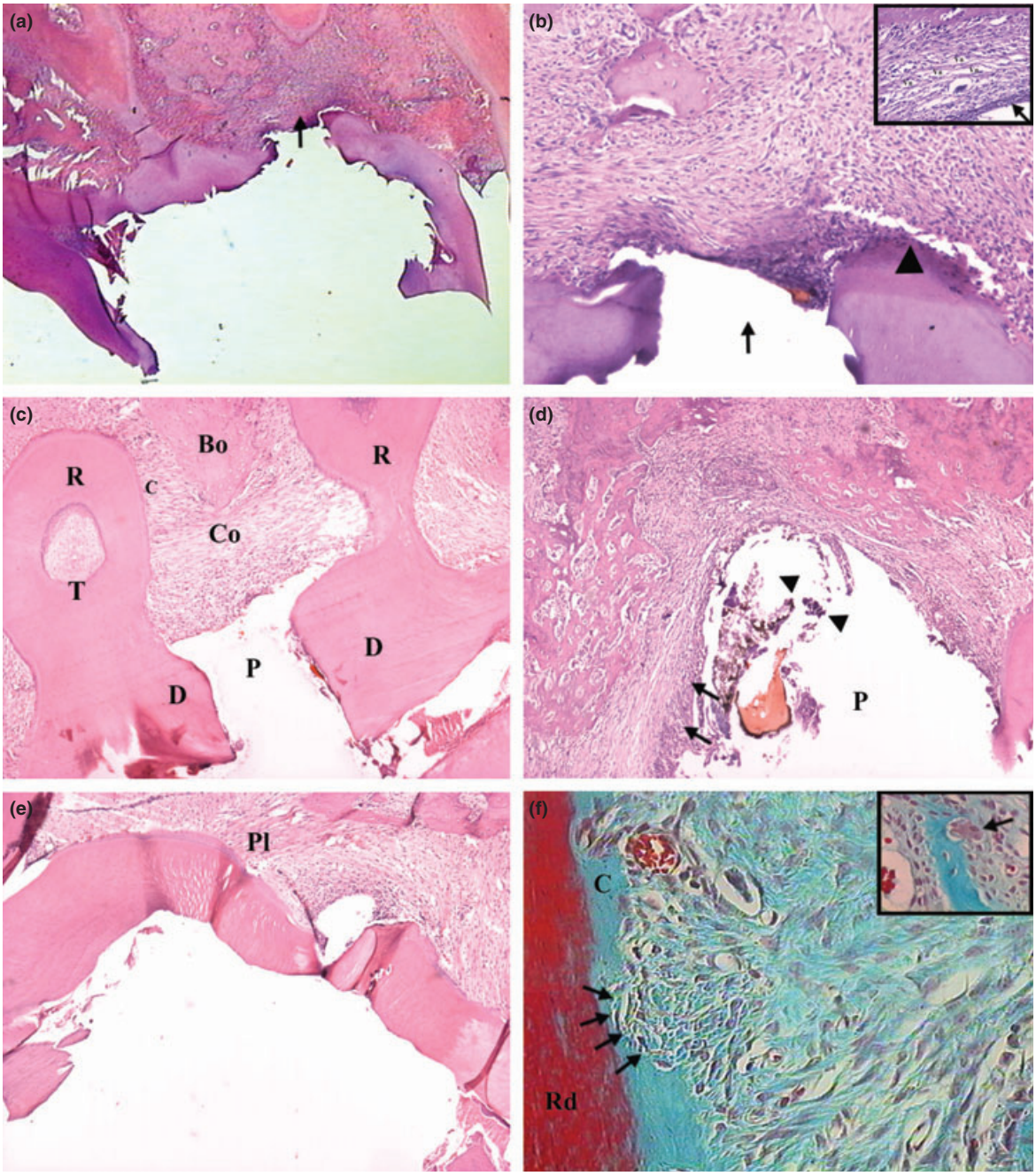

Figure 2 Histological aspects of the rat furcal lesion. (a) Day 14 post-surgery, perforation area showing granulation tissue (arrow). (b) Higher magnification of (a) inflammatory cells at the periphery of the perforation and disorganization of periodontal ligament (inset, arrow), the perforation site (arrow) and MTA fragments (arrow heads). (c) and (e) day 21 and 28, respectively showing the evolution of lesion towards repair (d) MTA-treated perforation at day 21, residues of MTA are present (arrows heads), notice the granulation tissue at the border of the perforation (arrows). (f) Intense vascular neorformation and deposition of collagen in the periodontal tissue, cement reabsorption (arrows), and osteoclastic activity (inset, arrow). C, cement; Co, collagen deposition T, pulp tissue; R, root; Bo, inter root bone D, dentine; P, perforation; Pl, periodontal ligament. (a), (c), (d) and (e) H&E, ×100; (b), H&E, ×200; (f) Gomori's trichome, ×400 and insets, ×400.

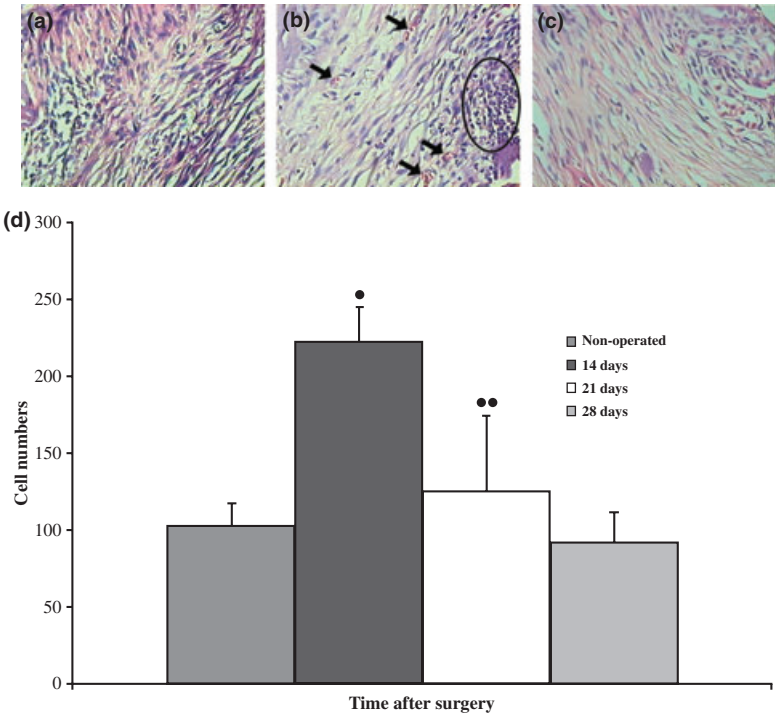

Figure 3 (a), (b) and (c) show, respectively, the intensity of periodontal tissue cellularity on days 14, 21 and 28 post-surgery. Also notice the presence of vascular congestion (small black arrows) and polimorfonuclear cells (encircled) on day 21 (H&E, ×400); (d) Morphometry of furcal lesion periodontal tissue. The graphic shows the average of cell numbers counted in two fields per animal sample at 400× magnification, at each time point. Data are presented as mean values of counted cells in each animal ($n = 3$). • Statistically significant difference ($P < 0.05$) between data from the non-operated group and the operated group 14 days post-surgery. •• Statistically significant difference ($P < 0.05$) between data from the operated groups on days 14 and 21 post-surgery.

of the perforation will help to facilitate the repair procedure (Daoudi & Saunders 2002). Hence, a model that simulates as much as possible the human clinical situation is crucial to the systematic assessment of the many biological aspects involved in this procedural accident.

In this study, all efforts were undertaken to reproduce the clinical conditions in an experimental model. Thus, the design of the stainless steel clamp was modified to increase its ability to completely grasp the tooth (Sampaio 1967). All surgical procedures were performed under aseptic conditions, since a rubber dam could isolate the tooth in a similar fashion to the practice in humans.

It should be recognized that the inflammatory response in rodents is different from that found in humans, however, the rat was selected as a model because the periodontal anatomy, the development of plaque and histopathology of the periodontal lesion in this animal is similar to that found in humans (Klausen 1991, Genco *et al.* 1998). Other advantages include knowledge of animal age, genetic background, and the ethical and economical issues that contraindicate the choice of large animals for research (Beavers *et al.* 1986, Balla *et al.*1991, Arens & Torabinejad 1996, Bramante *et al.* 2004). In addition, the rat model provides good access to the tooth and allows visibility of the surgical field. As manipulation of genetic and pharmacological parameters is possible in the rat, the establishment of this model will allow further studies on furcal perforation.

Histopathological results demonstrated the effects of the furcal lesion on the periodontal tissues. An increased number of polymorphonuclear cells at 14 day after surgery could be observed, counterbalanced by prevailing mononuclear cells on days 21 and 28. At 28 days, an increase of collagen deposition and an exuberance of granulation tissue were observed. Furthermore, morphometric assessments were in agreement with outcomes observed by previous workers (Balla *et al.* 1991,

Sousa *et al.* 2004) and showed an increase in inflammatory cell numbers around furcal perforations, which decreased with time. Other histological parameters such as periodontal ligament thickness, bone resorption area, collagen deposition could be accessed easily. Furthermore, despite its limitations this model was useful in accomplishing qualitative and quantitative (by morphometry) assessments.

It is well-known that failure of perforation repairs may be the result of the absence of a seal (Saunders & Saunders 1994). Therefore, in this study, perforations were sealed with MTA and histopatological analysis was performed. This is an example of the application of this model to analyse the biocompatibility aspects of sealing materials. The preliminary results presented here indicate that the presence of MTA may interfere positively with lesion progression. The assessment was taken on day 21 post-surgery, but further and systematic investigations are necessary.

The radiographic technique proposed revealed the anatomical structures of the normal periodontal and also demonstrated the adaptation of the filling materials, the perforation position and, in some cases, the destruction of interdental crest of bone. Alveolar bone mineral density was previously documented in mandibular radiographs and the film used was tested in rats previously (Xiong *et al.* 2007, Mahl & Fontanella 2008). Although morphometrical evaluation of alveolar bone loss was not documented, correlation between bone resorption and histological parameters has been described previously (Waterman *et al.*1998, Teixeira *et al.* 2000, Xiong *et al.* 2007).

Conclusion

This experimental animal model for furcal perforation is not totally comparable to human models of furcal lesions. However, under carefully standardized conditions, this model can be used to simulate the inflammatory process induced iatrogenically in humans during root canal treatment as an effective tool to study several aspects of tissue reaction to this specific kind of injury. Therefore, it is suitable for other studies on the triggering and control of the inflammatory reaction, as well as on the search for suitable sealing materials.

Acknowledgements

R.M.E. Arantes and L.Q. Vieira are supported by research fellowships from Conselho Nacional de Desenvolvimento Cientifico e Tecnológico (CNPq). This work was supported by grants from Fundação de Amparo à Pesquisa do Estado de Minas Gerais – FAPEMIG (CBB APQ-1323-3.13/07 and CNPq (grant number 350567/1995-6 and 571093/2008-6). The authors are indebted to the technicians Vânia Aparecida do Nascimento Silva for histopatological processing.

References

Al-Daafas A, Al-Nazhan S (2007) Histological evaluation of contaminated furcal perforation in dogs' teeth repaired by MTA with or without internal matrix. *Oral Surgery Oral Medicine Oral Pathology Oral Radiology and Endodontology* **103**, e92–9.

Arens DE, Torabinejad M (1996) Repair of furcal perforations with mineral trioxide aggregate: two case reports. *Oral Surgery Oral Medicine Oral Pathology Oral Radiology and Endodontology* **82**, 84–8.

Balla R, LoMonaco CJ, Skribner J, Lin LM (1991) Histological study of furcation perforations treated with tricalcium phosphate, hydroxylapatite, amalgam, and Life. *Journal of Endodontics* **17**, 234–8.

Beavers RA, Bergenholtz G, Cox CF (1986) Periodontal wound healing following intentional root perforations in permanent teeth of Macaca mulatta. *International Endodontic Journal* **19**, 36–44.

Bernabé PFE, Holland R (2004) Cirurgia paraendodôntica: como praticá-la com embasamento científico. In: Estrela C, *Ciência Endodôntica*, 3rd edn. Sao Paulo, Brazil: Artes Medicas, pp. 657–797.

Bhaskar SN, Rappaport HM (1971) Histologic evaluation of endodontic procedures in dogs. *Oral Surgery Oral Medicine Oral Pathology* **31**, 526–35.

Bramante CM, Berbert A, Bernardineli N, Gomes de Moraes I, Garcia RB (2004) *Acidentes e complicações no tratamento endodôntico: soluções clínicas*, 2nd edn. Sao Paulo, Brazil: Santos.

Caliari MV (1997) *Princípios Básicos de Morfometria Digital: KS300 para iniciantes*, Editora UFMG edn. Belo Horizonte, Minas Gerais, Brazil: UFMG.

Daoudi MF, Saunders WP (2002) In vitro evaluation of furcal perforation repair using mineral trioxide aggregate or resin modified glass lonomer cement with and without the use of the operating microscope. *Journal of Endodontics* **28**, 512–5.

Genco CA, Van DT, Amar S (1998) Animal models for Porphyromonas gingivalis-mediated periodontal disease. *Trends in Microbiology* **6**, 444–9.

Hartwell GR, England MC (1993) Healing of furcation perforations in primate teeth after repair with decalcified freeze-dried bone: a longitudinal study. *Journal of Endodontics* **19**, 357–61.

Klausen B (1991) Microbiological and immunological aspects of experimental periodontal disease in rats: a review article. *Journal of Periodontology* **62**, 59–73.

Mahl CR, Fontanella V (2008) Optimal parameters for lateral oblique radiographs of rat mandibles. *Dentomaxillofacial Radiology* **37**, 224–7.

Meister F, Lommel TJ, Gerstein H, Davies EE (1979) Endodontic perforations which resulted in alveolar bone loss. Report of five cases. *Oral Surgery Oral Medicine Oral Pathology* **47**, 463–70.

Möller AJR (1966) Microbiological examination of root canals and periapical tissues of human teeth. *Odontol Tidskr* **20**, 74–5.

Pacheco CMF, Queiroz-Junior CM, Maltos KLM *et al.* (2008) Crucial role of peripheral kappa-opioid receptors in a model of periodontal disease in rats. *Journal of Periodontal Research* **43**, 730–6.

Sampaio P (1967) Placement of a rubber dam on rat molars. *Journal of Dental Research* **46**, 1102.

Saunders WP, Saunders EM (1994) Coronal leakage as a cause of failure in root-canal therapy: a review. *Endodontics & Dental Traumatology* **10**, 105–8.

Seltzer RE, Bender IB (1990) *The Dental Pulp*, 3rd edn. Philadelphia: JB Lippincott.

Sousa CJ, Loyola AM, Versiani MA, Biffi JC, Oliveira RP, Pascon EA (2004) A comparative histological evaluation of the biocompatibility of materials used in apical surgery. *International Endodontic Journal* **37**, 738–48.

Teixeira FB, Gomes BP, Ferraz CC, Souza-Filho SC, Zaia AA (2000) Radiographic analysis of the development of periapical lesions in normal rats, sialoadenectomized rats and sialoadenectomized-immunosuppressed rats. *Dental Traumatology* **16**, 154–7.

Vajrabhaya LO, Korsuwannawong S, Jantarat J, Korre S (2006) Biocompatibility of furcal perforation repair material using cell culture technique: Ketac Molar versus ProRoot MTA. *Oral Surgery Oral Medicine Oral Pathology Oral Radiology and Endodontology* **102**, e48–50.

Walton RE, Torabinejad M (2002) *Principles and Practice of Endodontics*, 3rd edn. Oxford, UK: W B Saunders Co.

Waterman PA, Torabinejad M, McMillan PJ, Kettering JD (1998) Development of periradicular lesions in immunosuppressed rats. *Oral Surgery Oral Medicine Oral Pathology Oral Radiology and Endodontology* **85**, 720–5.

Wu MK, van der Sluis LW, Wesselink PR (2005) The risk of furcal perforation in mandibular molars using Gates-Glidden drills with anticurvature pressure. *Oral Surgery Oral Medicine Oral Pathology Oral Radiology and Endodontology* **99**, 378–82.

Xiong H, Peng B, Wei L, Zhang X, Wang L (2007) Effect of an estrogen-deficient state and alendronate therapy on bone loss resulting from experimental periapical lesions in rats. *Journal of Endodontics* **33**, 1304–8.

Supporting Information

Additional Supporting Information may be found in the online version of this article:

Video Clip S1. A video animation was designed using the blender software (Blender Foundation, Amsterdam, the Netherlands) to represent the entire surgical procedure. The video clip is in avi format.

Please note: Wiley-Blackwell are not responsible for the content or functionality of any supporting materials supplied by the authors. Any queries (other than missing material) should be directed to the corresponding author for the article.